

Contribution from the Departments of Chemistry, The Chung-Cheng Institute of Technology, Taiwan, Republic of China, and The University of Mississippi, University, Mississippi 38677

Preparation and Characterization of $K_xM^{II}_xM^{III}_{1-x}F_3$ ($x \approx 0.4-0.6$; $M^{II} = Mn, Ni$; $M^{III} = V, Cr$)

Y. S. Hong,[†] R. F. Williamson,[‡] K. N. Baker,[‡] T. Y. Du,[‡] S. M. Seyedahmadian,[‡] and W. O. J. Boo^{*‡}

Received September 27, 1991

The compounds $K_xM^{II}_xM^{III}_{1-x}F_3$ ($x \approx 0.4-0.6$; $M^{II} = Mn, Ni$; $M^{III} = V, Cr$) were prepared and studied. The tetragonal tungsten bronze structure formed for $M^{II} = Mn$ and $M^{III} = V, Cr$, and the modified pyrochlore structure formed for $M^{II} = Ni$ and $M^{III} = V, Cr$, except for $K_{0.60}Ni_{0.60}Cr_{0.40}F_3$, which formed the tetragonal bronze structure. From their magnetic behavior, we conclude that all of the tetragonal bronze compounds are ionically ordered and belong to space group $P4_2bc$ (C_{4v}^8). Magnetic ordering in these compounds occurs in two steps. Linear trimers (M^{II})³ and (M^{III})³ form first, giving rise to a quasi-paramagnetic region, followed at lower temperatures by long-range magnetic ordering. The $180^\circ M^{2+}-F-M^{3+}$ magnetic interactions appear to be ferromagnetic. Samples of compositions $Na_{0.25}K_{0.25}M^{II}_{0.50}M^{III}_{0.50}F_3$ and $Na_{0.50}M^{II}_{0.50}M^{III}_{0.50}F_3$ were also prepared and studied.

Introduction

Magneli¹ reported the structure of tetragonal tungsten bronze, K_xWO_3 ($x = 0.4-0.6$), to belong to space group $P4/mbm$ (D_{4h}^5). In this structure, tungsten ions are indistinguishable and occupy both 8j and 2c sites. Banks, Nakajima, and Williams² reported that $K_{0.54}Mn_{0.54}Fe_{0.46}F_3$ belongs to space group $P4_2bc$ (C_{4v}^8). This lowering of symmetry is a consequence of ionic ordering of Mn^{2+} and Fe^{3+} in the fluoride analogue. The Mn^{2+} ions are found on one set of 8c sites, designated M(1), and Fe^{3+} ions are found on a second set of 8c sites, designated M(2). Both Mn^{2+} and Fe^{3+} ions randomly occupy 4b sites, designated M(3).

Mounting evidence indicates that ionic ordering of the type found in $K_{0.54}Mn_{0.54}Fe_{0.46}F_3$ is common in fluoride analogues of tungsten bronze. From their magnetic behavior, we have concluded that K_xVF_3 and $K_xMn_xCr_{1-x}F_3$,⁴ as well as $K_xMn_xFe_{1-x}F_3$,⁵ belong to space group $P4_2bc$ (C_{4v}^8) over their entire composition spans ($x \approx 0.4-0.6$). Only the occupation of 4b sites is affected by composition change. At $x = 0.50$, occupation of the 4b sites is random in the *ab* plane; however, M^{2+} and M^{3+} ions on 4b sites along the *c* direction are ordered.

The ionically ordered structure of $K_{0.50}M^{II}_{0.50}M^{III}_{0.50}F_3$ in the *ab* plane is illustrated on Figure 1. The magnetic data has also allowed us to make quantitative conclusions regarding the magnitude and sign of the magnetic exchange constant, *J*, between neighboring paramagnetic ions. All near-neighbor interactions in the tetragonal bronze structure are approximately 180° , and for $K_{0.50}M^{II}_{0.50}M^{III}_{0.50}F_3$, the interactions $M^{2+}-F-M^{2+}$, $M^{3+}-F-M^{3+}$, and $M^{2+}-F-M^{3+}$ occur in the ratio 1:1:13. From their magnetic susceptibilities, we deduced for KV_2F_6 $|J_{2+,2+}| \approx |J_{2+,3+}| \approx |J_{3+,3+}|$,³ for $KMnFeF_6$ $|J_{3+,3+}| > |J_{2+,3+}| > |J_{2+,2+}|$,⁵ and for $KMnCrF_6$ $|J_{2+,2+}| \approx |J_{3+,3+}| \gg |J_{2+,3+}|$.⁴ Furthermore, all of the magnetic interactions in these compounds are antiferromagnetic except $J_{2+,3+}$ in $K_{0.50}Mn_{0.50}Cr_{0.50}F_3$ (i.e., $Mn^{2+}-F-Cr^{3+}$), which is weakly ferromagnetic.

We reported the magnetic properties of the trirutile compound $LiMnVF_6$.⁶ In the trirutile structure as in the rutile structure, there are two important magnetic interactions: J_1 , between nearest-neighbor metal ions, and J_2 , between second-nearest neighbors. In this compound, $|J_1| \gg |J_2|$; hence, magnetic ordering occurs in steps: dimers form first between nearest-neighbor (Mn,V) pairs, and three-dimensional, long-range ordering occurs at a lower temperature. One of the interesting features of this mechanism is the existence of a quasi-paramagnetic region at temperatures where the dimers are stable but above the temperature at which long-range magnetic ordering sets in. In a plot of χ^{-1} vs *T*, this quasi-paramagnetic behavior is supported by the existence of a second linear region.

In $KMnCrF_6$, a situation exists similar to that in $LiMnVF_6$. The ionic ordering displayed on Figure 1 reveals that if a M(3)

site is occupied by a Mn^{2+} ion, it has two nearest-neighbor Mn^{2+} ions on M(1) sites or if a M(3) site is occupied by a Cr^{3+} ion, it has two nearest-neighbor Cr^{3+} ions on M(2) sites. Since the (Mn,Mn) and (Cr,Cr) magnetic interactions are believed to be much stronger than the (Mn,Cr) interactions, we conclude that magnetically-coupled linear trimers, (Mn)³ and (Cr)³, form first, followed by three-dimensional, long-range ordering at a lower temperature. Only 6 of every 10 metal ions would form trimers, one (Mn)³ and one (Cr)³. Since the magnetic interactions within these trimers are known to be antiferromagnetic, the resultant spin moments of (Mn)³ and (Cr)³ would be $5/2$ and $3/2$, respectively. Of the 10 metal ions the number of species with resultant spins of $5/2$ would be 3 [one (Mn)³ and two Mn^{2+}] and the number with spins of $3/2$ would also be 3 [one (Cr)³ and two Cr^{3+}]. Therefore, a quasi-paramagnetic temperature region should exist below the temperatures where the trimers are formed but above the temperature at which long-range ordering sets in, with a C_M' value quantitatively equal to $0.6 C_M$. To establish the existence of the quasi-paramagnetic region, we have remeasured the magnetic susceptibility of $K_{0.50}Mn_{0.50}Cr_{0.50}F_3$ over smaller temperature intervals.

Assuming that other fluoride analogues of tetragonal tungsten bronze will be ionically ordered as illustrated on Figure 1, the rules of Goodenough⁷ and Kanamori⁸ make it possible to select combinations of first-row transition metal ions which may become magnetically ordered in two steps and may even demonstrate ferromagnetic behavior. In addition to remeasuring (Mn,Cr), we have chosen to prepare and study the phase systems $K_xM^{II}_xM^{III}_{1-x}F_3$ ($x = 0.4-0.6$) with combinations (Mn,V), (Ni,Cr), and (Ni,V).

Babel, Pausewang, and Viebahn⁹ reported that $K_{0.50}Ni_{0.50}Cr_{0.50}F_3$ ($KNiCrF_6$) crystallizes in the modified pyrochlore structure. Babel¹⁰ later demonstrated that when $KNiF_3$ is reacted with CrF_3 at $800^\circ C$, under a pressure of 30 kbar, the product has the tetragonal tungsten bronze structure. Since these authors only reported samples of composition $x = 0.50$, we elected to examine the phase system from $x = 0.40$ to 0.60 in the event that

- (1) Magneli, A. *Ark. Kemi* **1949**, *1*, 213.
- (2) Banks, E.; Nakajima, S.; Williams, G. J. B. *Acta Crystallogr.* **1979**, *B35*, 46.
- (3) Hong, Y. S.; Williamson, R. F.; Boo, W. O. J. *Inorg. Chem.* **1980**, *19*, 2229.
- (4) Banks, E.; Shone, M.; Hong, Y. S.; Williamson, R. F.; Boo, W. O. J. *Inorg. Chem.* **1982**, *21*, 3894.
- (5) Banks, E.; Shone, M.; Williamson, R. F.; Boo, W. O. J. *Inorg. Chem.* **1983**, *22*, 3339.
- (6) Williamson, R. F.; Arafat, E. S.; Baker, K. N.; Rhee, C. H.; Sanders, J. R.; Scheffler, T. B.; Zeidan, H. S.; Boo, W. O. J. *Inorg. Chem.* **1985**, *24*, 482.
- (7) Goodenough, J. B. *Magnetism and the Chemical Bond*; Interscience: New York, 1963; pp 165-185.
- (8) Kanamori, J. *Phys. Chem. Solids* **1959**, *10*, 87.
- (9) Babel, D.; Pausewang, G.; Viebahn, W. *Z. Naturforsch.* **1967**, *22B*, 1219.
- (10) Babel, D. *Z. Anorg. Allg. Chem.* **1972**, *387*, 161.

* Author to whom correspondence should be addressed.

[†] The Chung-Cheng Institute of Technology.

[‡] The University of Mississippi.

Table I. Lattice and Magnetic Constants

compd	lattice const (±0.05%), Å	T_N , K	θ , K	C_M , cm ³ deg mol ⁻¹		σ_0 , μ_B
				obsd	calcd	
$K_{0.50}Mn_{0.50}Cr_{0.50}F_3$	$a = 12.649$ $c = 7.935$	31	$\theta = 0$ $\theta' = 19$	$C_M = 3.13$ $C_M' = 1.99$	3.10 1.86	1.90
$K_{0.44}Mn_{0.44}V_{0.56}F_3$	$a = 12.681$ $c = 7.860$	12	$\theta = -18$ $\theta' = -1.5$	$C_M = 2.14$ $C_M' = 1.43$	2.35	0.12
$K_{0.45}Mn_{0.45}V_{0.55}F_3$	$a = 12.701$ $c = 7.862$	19	$\theta = -19$ $\theta' = +1.5$	$C_M = 2.30$ $C_M' = 1.50$	2.39	0.08
$K_{0.50}Mn_{0.50}V_{0.50}F_3$	$a = 12.718$ $c = 7.916$	21	$\theta = -16$ $\theta' = +3$	$C_M = 2.51$ $C_M' = 1.50$	2.57 1.54	0.12
$K_{0.55}Mn_{0.55}V_{0.45}F_3$	$a = 12.795$ $c = 7.998$	21	$\theta = -30$ $\theta' = +6.5$	$C_M = 2.66$ $C_M' = 1.37$	2.75	0.18
$K_{0.60}Mn_{0.60}V_{0.40}F_3$	$a = 12.845$ $c = 8.052$	24	$\theta = -43$ $\theta' = +3.5$	$C_M = 2.74$ $C_M' = 1.22$	2.93	0.13
$K_{0.40}Ni_{0.40}Cr_{0.60}F_3$	$a = 10.294$		$\theta = -82$	$C_M = 2.47$	1.59	0
$K_{0.45}Ni_{0.45}Cr_{0.55}F_3$	$a = 10.258$		$\theta = -58$	$C_M = 2.11$	1.56	0
$K_{0.50}Ni_{0.50}Cr_{0.50}F_3$	$a = 10.236$		$\theta = -40$	$C_M = 1.54$	1.53	0
$K_{0.55}Ni_{0.55}Cr_{0.45}F_3$	$a = 10.225$		$\theta = -38$	$C_M = 1.45$	1.50	0
$K_{0.60}Ni_{0.60}Cr_{0.40}F_3$	$a = 12.450$ $c = 7.822$	63	$\theta = 15$ $\theta' = 30$	$C_M = 1.41$ $C_M' = 1.22$	1.47	0
$K_{0.40}Ni_{0.40}V_{0.60}F_3$	$a = 10.403$					
$K_{0.45}Ni_{0.45}V_{0.55}F_3$	$a = 10.398$					
$K_{0.50}Ni_{0.50}V_{0.50}F_3$	$a = 10.382$		$\theta = -80$	$C_M = 0.92$	1.00	0
$K_{0.55}Ni_{0.55}V_{0.45}F_3$	$a = 10.366$					
$K_{0.60}Ni_{0.60}V_{0.40}F_3$	$a = 10.531$					
$Na_{0.25}K_{0.25}Mn_{0.50}Cr_{0.50}F_3$	$a = 12.518$ $c = 7.807$	20	$\theta = -13$ $\theta' = +10$	$C_M = 2.82$ $C_M' = 1.76$	3.10 1.86	0.87
$Na_{0.25}K_{0.25}Ni_{0.50}Cr_{0.50}F_3$	$a = 10.272$					

IONIC ORDERING

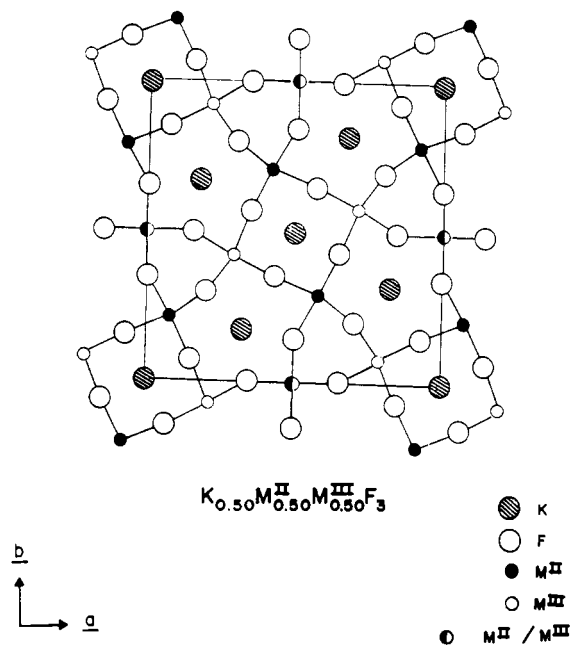


Figure 1. Ionically ordered structure of $K_{0.50}M^{II}_{0.50}M^{III}_{0.50}F_3$. M^{II} ions occupy M(1) sites, M^{III} ions occupy M(2) sites, and M(3) sites are occupied by either M^{II} or M^{III} ions.

the tetragonal bronze structure might form at either extremity. The systems $K_xMn_xV_{1-x}F_3$ and $K_xNi_xV_{1-x}F_3$ ($x = 0.40-0.60$) have not been previously reported.

The modified pyrochlore structure usually forms for compounds of composition $Rb_{0.50}M^{II}_{0.50}M^{III}_{0.50}F_3$ or $Cs_{0.50}M^{II}_{0.50}M^{III}_{0.50}F_3$, but it is curious that it forms for $K_{0.50}M^{II}_{0.50}M^{III}_{0.50}F_3$, since the K^+ ion is small. The modified pyrochlore structure may be thought of as a geometrical packing of tetrahedra and truncated tetrahedra in the ratio 1:1 where the M^{2+} and M^{3+} ions are located at all vertices of the polyhedra and F^- ions are located approximately in the centers of the edges of the polyhedra. The alkali metal ions Rb^+ and Cs^+ are known to occupy the truncated tetrahedral sites, but there is some question as to where the K^+ ions might reside. To answer some questions regarding the size effect of the alkali

metal ions on structure, we have included studies of the compounds $Na_{0.25}K_{0.25}M^{II}_{0.50}M^{III}_{0.50}F_3$ and $Na_{0.50}M^{II}_{0.50}M^{III}_{0.50}F_3$ ($M^{II} = Mn, Ni$; $M^{III} = V, Cr$).

Experimental Section

The magnetic susceptibility of $K_{0.50}Mn_{0.50}Cr_{0.50}F_3$ was remeasured from 4.2 to 70 K at temperature intervals of approximately 2 K.

Samples of $K_xMn_xV_{1-x}F_3$, $K_xNi_xCr_{1-x}F_3$, and $K_xNi_xV_{1-x}F_3$ ($x = 0.40, 0.45, 0.50, 0.55, 0.60$), as well as samples of compositions $Na_{0.25}K_{0.25}M^{II}_{0.50}M^{III}_{0.50}F_3$ and $Na_{0.50}M^{II}_{0.50}M^{III}_{0.50}F_3$ ($M^{II} = Mn, Ni$; $M^{III} = V, Cr$), were prepared and studied. Stoichiometric amounts of NaF, KF, MF_2 , and MF_3 were vacuum encapsulated inside molybdenum containers. The $K_xM^{II}_xM^{III}_{1-x}F_3$ samples were prepared in 3.2 cm long \times 1.9 cm diameter containers, and the other samples in 3.2 cm long \times 0.65 cm diameter containers. The sealed Mo containers were fired at 850 °C for 14 days. Weight checks were made after each step to ensure that compositions of products were unchanged from nominal values. All samples were examined by optical microscopy for homogeneity and impurities to assure there was no reaction between the products and the container material. X-ray powder diffraction data were obtained by Guinier-Hagg techniques using $Cu K\alpha_1$ radiation and Si as an internal standard. Precision lattice constants were determined by least-squares analyses.

Magnetic susceptibility measurements were made from 4.2 to 300 K and between 0 and 10 kG with a Foner type PAR vibrating-sample magnetometer equipped with a Janis liquid-helium dewar and gallium arsenide temperature controller. Magnetic fields were measured with an F.W. Bell Hall-probe gaussmeter, Model 8860. Corrections for core diamagnetism were made from ionic susceptibility tables of Mulay.¹¹

Results

$K_{0.50}Mn_{0.50}Cr_{0.50}F_3$. A plot of χ^{-1} vs T from the remeasured susceptibility of $K_{0.50}Mn_{0.50}Cr_{0.50}F_3$, over the range 4.2–70 K is shown on Figure 2. This figure clearly shows a linear region between 25 and 50 K with $C_M' = 1.99$ and $\theta' = 19$ K. The ratio $C_M'/C_M = 0.636$. The lattice and magnetic parameters of $K_{0.50}Mn_{0.50}Cr_{0.50}F_3$ are given in Table I. The parameters include T_N (long-range magnetic ordering temperature), θ and C_M (Curie-Weiss constants obtained from the high-temperature paramagnetic region), θ' and C_M' (Curie-Weiss constants from the quasi-paramagnetic region), and σ_0 (the spontaneous magnetic moment).

$K_xMn_xV_{1-x}F_3$. Optical and X-ray analyses indicate the samples of nominal composition $K_{0.45}Mn_{0.45}V_{0.55}F_3$, $K_{0.50}Mn_{0.50}V_{0.50}F_3$,

(11) Mulay, L. N. *Magnetic Susceptibility*; Interscience: New York, 1963; p 1782.

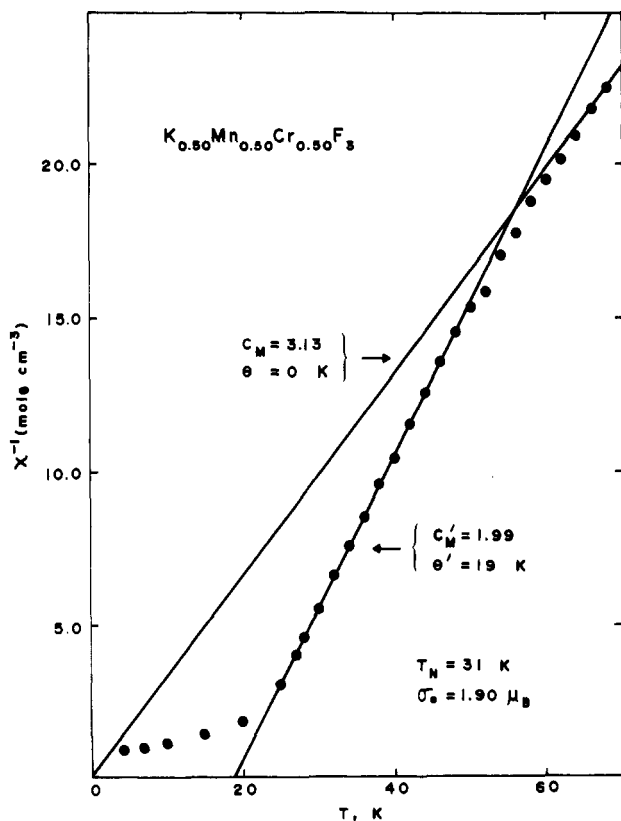


Figure 2. Inverse magnetic susceptibility of $K_{0.50}Mn_{0.50}Cr_{0.50}F_3$ vs temperature from 4.2 to 70 K.

$K_{0.55}Mn_{0.55}V_{0.45}F_3$, and $K_{0.60}Mn_{0.60}V_{0.40}F_3$ to be homogeneous and single phased. The color of the samples was light green. All X-ray diffraction lines of these four samples were fitted to tetragonal tungsten bronze type structures. The sample $K_{0.40}Mn_{0.40}V_{0.60}F_3$ contained two phases. Most of this sample consisted of a tetragonal tungsten bronze phase, with a small amount of a hexagonal tungsten bronze phase. X-ray results of the five samples are shown in Table I.

The range of chemical composition of the tetragonal phase was determined to be $x = 0.44$ – 0.60 from a linear plot of the interlayer distances, c' , vs $-\log x$ (Figure 3). The previously reported values of c' for $K_xMn_xCr_{1-x}F_3$ are included on the same plot for comparison.

Magnetic susceptibilities of the five powdered samples were similar, and none displayed a maximum over the temperature range 4.2–300 K. All five samples, however, displayed small spontaneous magnetic moments at low temperatures, which allowed us to determine T_N values. The inverse susceptibility vs T and magnetic moments extrapolated to zero field, σ , vs T of a powdered sample of $K_{0.50}Mn_{0.50}V_{0.50}F_3$ are shown on Figure 4. As was the case for $K_xMn_xCr_{1-x}F_3$, the $K_xMn_xV_{1-x}F_3$ compounds display two linear regions.

$K_xNi_xCr_{1-x}F_3$. The samples of $K_xNi_xCr_{1-x}F_3$ formed the cubic, modified pyrochlore structure for $x = 0.40, 0.45, 0.50$, and 0.55 . The value of a for $K_{0.50}Ni_{0.50}Cr_{0.50}F_3$ is within reasonable agreement with that published by Babel et al.⁹ The sample $K_{0.60}Ni_{0.60}Cr_{0.40}F_3$ formed the tetragonal bronze structure. Optical and X-ray analyses indicated the samples of composition $x = 0.40, 0.45$, and 0.50 were homogeneous and single phased. The sample of composition $x = 0.55$ was primarily cubic but contained less than 1% of the tetragonal bronze phase, while the sample $x = 0.60$, which was primarily tetragonal, contained small amounts of the cubic modified pyrochlore phase. All five samples were bright green in color. Lattice dimensions are shown in Table I.

A plot of densities calculated from the X-ray data vs x was found to be linear for the modified pyrochlore phase (Figure 5), which established a check that the composition of this phase exists within the range $x = 0.40$ – 0.55 .

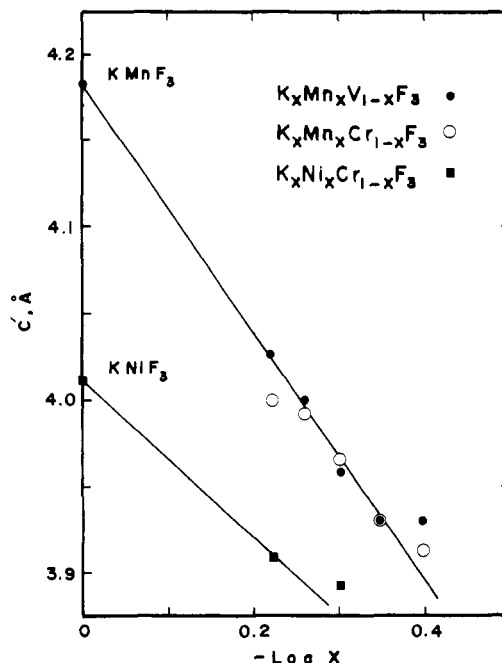


Figure 3. Linear plots of interlayer distances, c' , vs $-\log x$ for the $K_xMn_xV_{1-x}F_3$, $K_xMn_xCr_{1-x}F_3$, and $K_xNi_xCr_{1-x}F_3$ compounds.

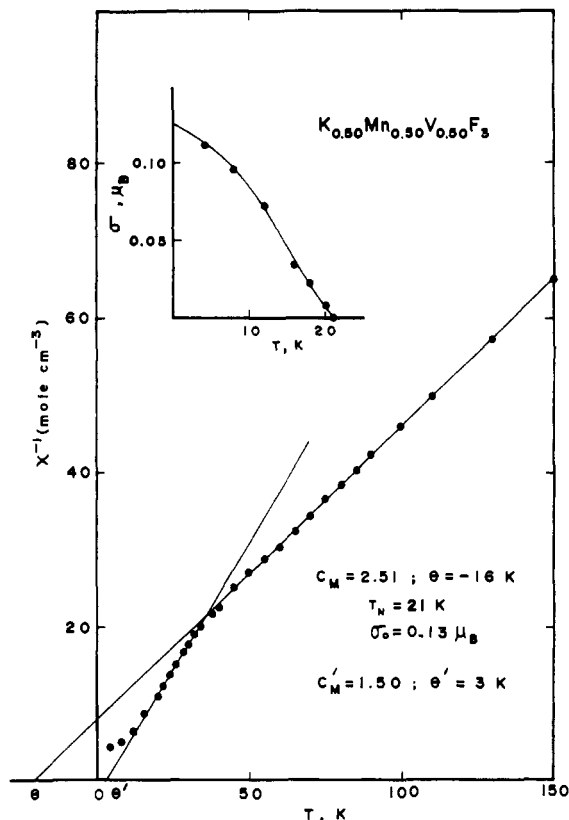


Figure 4. Inverse susceptibility vs temperature and magnetic moments extrapolated to zero field vs temperature for $K_{0.50}Mn_{0.50}V_{0.50}F_3$.

The interlayer distances, c' , vs $-\log x$ of $K_{0.60}Ni_{0.60}Cr_{0.40}F_3$, along with literature values for $KNiF_3$ ¹² and the tetragonal tungsten bronze phase $K_{0.50}Ni_{0.50}Cr_{0.50}F_3$ ¹⁰ formed under high pressure, are shown on Figure 3.

The magnetic susceptibilities of the modified pyrochlore samples ($x = 0.40, 0.45, 0.50, 0.55$) from 4.2 to 300 K appeared similar. None displayed spontaneous magnetic moments or showed other evidence of magnetic ordering above 4.2 K. Figure 6 shows the

(12) Knox, K. *Acta Crystallogr.* 1961, 14, 583.

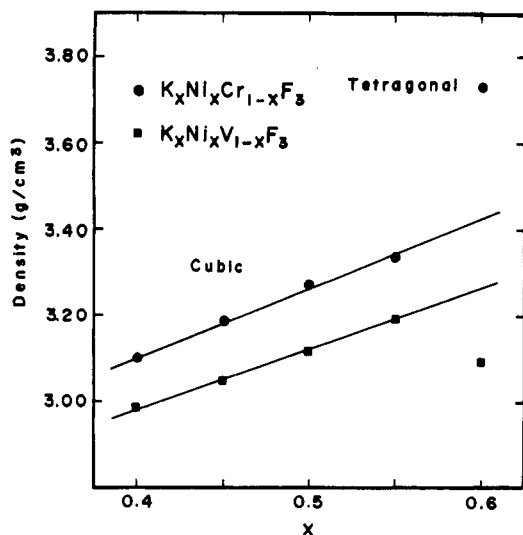


Figure 5. Linear plots of calculated density vs x for $K_xNi_xCr_{1-x}F_3$ and $K_xNi_xV_{1-x}F_3$.

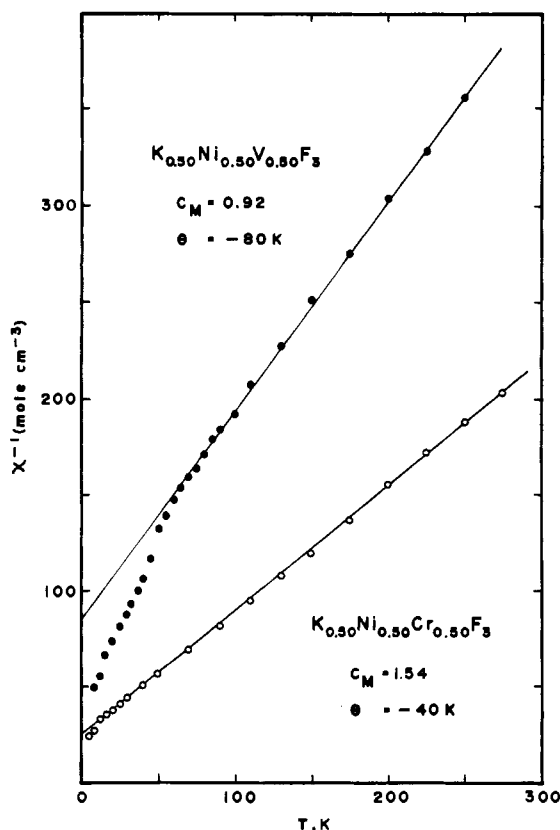


Figure 6. Inverse susceptibilities vs temperature for $K_{0.50}Ni_{0.50}V_{0.50}F_3$ and $K_{0.50}Ni_{0.50}Cr_{0.50}F_3$.

plot of χ^{-1} vs T for $K_{0.50}Ni_{0.50}Cr_{0.50}F_3$.

The magnetic susceptibility of $K_{0.60}Ni_{0.60}Cr_{0.40}F_3$ passes through a maximum at 63 K. A plot of χ^{-1} vs T (Figure 7) displays two linear regions, one above 150 K and a second between 63 and 150 K. The magnetic parameters of the five $K_xNi_xCr_{1-x}F_3$ samples are included in Table I.

$K_xNi_xV_{1-x}F_3$. Optical and X-ray analyses indicate all of the $K_xNi_xV_{1-x}F_3$ samples ($x = 0.40, 0.45, 0.50, 0.55, 0.60$) to be homogeneous, single phased, and cubic. The color of the five samples was bright green. All X-ray diffraction lines of these samples were fitted to a cubic, modified pyrochlore structure. The X-ray data for $K_{0.60}Ni_{0.60}V_{0.40}F_3$, however, showed the additional weak lines (211), (310), (520), (722), and (730). These lines do not obey the conditions, all hkl odd or all hkl even, required of a face-centered lattice. A plot of calculated density vs x for the

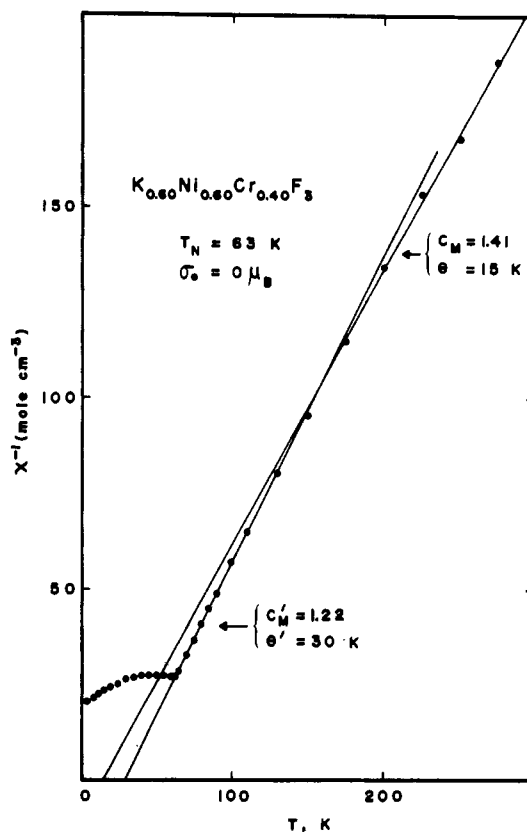


Figure 7. Inverse susceptibility vs temperature for $K_{0.60}Ni_{0.60}Cr_{0.40}F_3$.

$K_xNi_xV_{1-x}F_3$ compounds is included on Figure 5.

The magnetic susceptibility of $K_{0.50}Ni_{0.50}V_{0.50}F_3$ does not pass through a maximum between 4.2 and 300 K. A plot of χ^{-1} vs T is included on Figure 6. The region between 4.2 and 75 K was measured twice, and although this region appears linear on Figure 6, it really has distinct curvatures. The lattice constants for all of the $K_xNi_xV_{1-x}F_3$ compounds, and the magnetic constants for $K_{0.50}Ni_{0.50}V_{0.50}F_3$, are disclosed in Table I.

$Na_{0.25}K_{0.25}M^{II}_{0.50}M^{III}_{0.50}F_3$ ($M^{II} = Mn, Ni; M^{III} = Cr, V$). Homogeneous, single-phased compounds did not form for the compositions $M^{II} = Mn, M^{III} = V$ and $M^{II} = Ni, M^{III} = V$, but the compounds $Na_{0.25}K_{0.25}Mn_{0.50}Cr_{0.50}F_3$ and $Na_{0.25}K_{0.25}Ni_{0.50}Cr_{0.50}F_3$ each formed homogeneous, single-phased, green material. Optical and X-ray analyses revealed the former compound to have the tetragonal tungsten bronze structure (like $K_{0.50}Mn_{0.50}Cr_{0.50}F_3$) and the latter compound to have a modified pyrochlore type structure (similar to $K_{0.50}Ni_{0.50}Cr_{0.50}F_3$). The X-ray powder data for $Na_{0.25}K_{0.25}Ni_{0.50}Cr_{0.50}F_3$ contained a few weak lines which did not obey the conditions hkl all odd or all even. The magnetic constants for $Na_{0.25}K_{0.25}Mn_{0.50}Cr_{0.50}F_3$ are in Table I.

$Na_{0.50}M^{II}_{0.50}M^{III}_{0.50}F_3$ ($M^{II} = Mn, Ni; M^{III} = V, Cr$). Homogeneous, single-phased compounds formed for $M^{II} = Mn$ and $M^{III} = V, Cr$. All X-ray powder diffraction lines of these compounds were indexed to hexagonal unit cells ($Na_{0.50}Mn_{0.50}Cr_{0.50}F_3$, $a_{hex} = 9.026 \text{ \AA}$, $c_{hex} = 4.993 \text{ \AA}$; $Na_{0.50}Mn_{0.50}F_3$, $a_{hex} = 8.9714 \text{ \AA}$, $c_{hex} = 5.058 \text{ \AA}$). The lattice dimensions of $Na_{0.50}Mn_{0.50}Cr_{0.50}F_3$ are in excellent agreement with those reported by Courbion, Jacoboni, and DePape.¹³

Single-phased compounds did not form for $M^{II} = Ni$ and $M^{III} = V, Cr$. The predominant phase in each of these samples had a websterite type structure.

Discussion

Tetragonal Tungsten Bronze Phases. The tetragonal tungsten bronze phase forms for $K_xMn_xCr_{1-x}F_3$ ($x = 0.42-0.57$),

(13) Courbion, G.; Jacoboni, C.; DePape, R. *Acta Crystallogr.* 1977, B33, 1405.

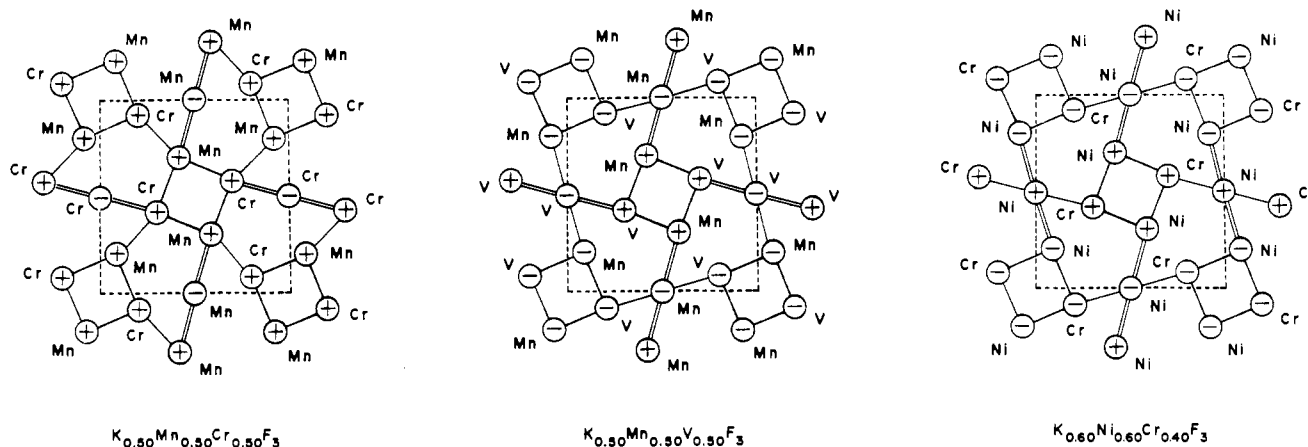


Figure 8. Proposed magnetic structures of $K_{0.50}Mn_{0.50}Cr_{0.50}F_3$, $K_{0.50}Mn_{0.50}V_{0.50}F_3$, and $K_{0.60}Ni_{0.60}Cr_{0.40}F_3$. Double bars represent antiferromagnetic coupling; single bars represent ferromagnetic coupling.

$K_xMn_xV_{1-x}F_3$ ($x = 0.44-0.60$), $K_xNi_xCr_{1-x}F_3$ (at $x = 0.60$), and for $Na_{0.25}K_{0.25}Mn_{0.50}Cr_{0.50}F_3$. The composition limits of the first two systems were determined from plots of c' vs $-\log x$. Magnetic data support the existence of similar $M^{2+}-M^{3+}$ ionic ordering in these compounds and that their structures belong to space group $P4_2bc$ (C_{4v}^8).

A plot of χ^{-1} vs T of $K_{0.50}Mn_{0.50}Cr_{0.50}F_3$ between 4.2 and 70 K (Figure 2) clearly indicates the region between 30 and 50 K is linear. The unit cell of $K_{0.50}Mn_{0.50}Cr_{0.50}F_3$ contains 10 Mn^{2+} ions and 10 Cr^{3+} ions. At about 60 K, relatively strong antiferromagnetic coupling between neighboring Mn^{2+} ions occurs forming linear trimers, $(Mn)^3$, with resultant spins of $5/2$. Coupling of Cr^{3+} ions occurs in this same temperature region forming linear trimers, $(Cr)^3$, with resultant spins of $3/2$. The formation of linear trimers reduces the number of each paramagnetic species from 10 to 6 (10 Mn^{2+} ions to 4 Mn^{2+} ions and 2 $(Mn)^3$ trimers, and 10 Cr^{3+} ions to 4 Cr^{3+} ions and 2 $(Cr)^3$ trimers). The fact that $C_M' \approx 0.60C_M$ supports the conclusion that a quasi-paramagnetic region exists between 30 and 50 K.

At 31 K, long-range magnetic order sets in as a result of (Mn,Cr) ferromagnetic coupling. A proposed magnetic structure for $K_{0.50}Mn_{0.50}Cr_{0.50}F_3$ is illustrated on Figure 8. Intratrimer coupling in $(Mn)^3$ and $(Cr)^3$ is antiferromagnetic, which is represented by double bars. Ferromagnetic coupling (Mn,Cr) is illustrated by single bars.

Magnetic ordering in $K_{0.50}Mn_{0.50}V_{0.50}F_3$ occurs in two steps, as in $K_{0.50}Mn_{0.50}Cr_{0.50}F_3$. However, we conclude that its long-range magnetic structure must be different from that of (Mn,Cr) , since it displays a relatively small spontaneous magnetic moment. In (Mn,V) , antiferromagnetic interactions form linear trimers, $(Mn)^3$ and $(V)^3$, near 40 K, with resultant spins of $5/2$ and 1, respectively. This gives rise to the quasi-paramagnetic region between 20 and 35 K seen on Figure 4. The ratio $C_M'/C_M = 0.598$ is remarkably close to the theoretical value of 0.6. The proposed magnetic structure of (Mn,V) is shown on Figure 8. Upon comparison of the proposed structures of (Mn,Cr) and (Mn,V) on Figure 8, it is conceivable that external magnetic fields may induce small magnetic moments in (Mn,V) .

At the composition $x = 0.50$, neighboring linear trimers along the crystallographic c axis should alternate $(M^{II})^3$, $(M^{III})^3$, $(M^{II})^3$, $(M^{III})^3$,... At compositions other than $x = 0.50$, the possibility exists for antiferromagnetic coupling between like trimers. The compositions $x = 0.40$ and 0.60 represent the extremes at which trimers are all $(M^{III})^3$ and all $(M^{II})^3$, respectively. Each of the five $K_xMn_xV_{1-x}F_3$ compounds were measured at small temperature intervals from 4.2 to 60 K, and each displays two linear regions on plots of χ^{-1} vs T . The large values of C_M' for $x \neq 0.50$ (Table I) suggests that coupling between like trimers along the c axis does not occur above T_N .

Of the five $K_xNi_xCr_{1-x}F_3$ samples, the tetragonal bronze structure formed only at $x = 0.60$. A plot of χ^{-1} vs T (Figure 7) is consistent with an ionically ordered structure upon which

magnetic coupling forms linear trimers, $(Ni)^3$, near 150 K. Two linear regions are present on Figure 7, and long-range magnetic ordering sets in at 63 K. No spontaneous magnetic moment was observed, but the positive θ' value (30 K) indicates that the $Ni^{2+}-F-Cr^{3+}$ interaction is ferromagnetic. A proposed magnetic structure for (Ni,Cr) is illustrated on Figure 8.

The plot of calculated density vs x for (Ni,Cr) , on Figure 5, shows the density of the cubic phase is considerably smaller than the tetragonal phase. This is consistent with Babel's experiment in which he formed the tetragonal phase under 30 kbar and 800 °C.¹⁰ However, we included Babel's c' value on Figure 3 and we believe the composition of this compound is not $x = 0.50$ but something between $x = 0.50$ and 0.60 .

The magnetic susceptibility measurements made on $Na_{0.25}K_{0.25}Mn_{0.50}Cr_{0.50}F_3$ indicate magnetic ordering behavior similar to that in $K_{0.50}Mn_{0.50}Cr_{0.50}F_3$. A plot of χ^{-1} vs T displays two linear regions with $C_M'/C_M = 0.624$ and a θ' value of +10 K. These features along with a sizable spontaneous moment ($0.87 \mu_B$) leads us to believe its magnetic structure is the same as (Mn,Cr) on Figure 8.

Modified Pyrochlore Phases. The modified pyrochlore phase forms for $K_xNi_xCr_{1-x}F_3$ ($x = 0.40-0.55$), $K_xNi_xV_{1-x}F_3$ ($x = 0.40-0.60$), and $Na_{0.25}K_{0.25}Ni_{0.50}Cr_{0.50}F_3$. The fact that these modified pyrochlore compounds are cubic suggests there is no $M^{2+}-M^{3+}$ ionic ordering.

The X-ray data shown in Table I reveal that the dimensions of the cubic unit cell decreased as x increases over the region $x = 0.40-0.55$. This effect is present in both (Ni,Cr) and (Ni,V) . The calculated density of these compounds was found to be linear with respect to x (Figure 5). The lattice dimensions and calculated density of $K_{0.60}Ni_{0.60}V_{0.40}F_3$, however, are dramatically different from these trends.

There are two possible sites in the modified pyrochlore structure for the K^+ ion: tetrahedral sites (with M coordination of 4) and truncated tetrahedral sites (with M coordination of 12). These sites occur in the ratio 1:1, and at $x = 0.50$, each truncated tetrahedral site is believed to contain one K^+ ion. At compositions above $x = 0.50$, some of the K^+ ions may occupy tetrahedral sites as well, and this would explain why the dimensions of the unit cell are larger for $x = 0.60$. Additional lines in the X-ray diffraction powder pattern ($x = 0.60$) suggests that the occupied tetrahedral sites are ordered, and this ordering lowers the symmetry of the crystal from face-centered cubic to primitive cubic.

The compound $Na_{0.25}K_{0.25}Ni_{0.50}Cr_{0.50}F_3$ displays structural behavior similar to $K_{0.60}Ni_{0.60}V_{0.40}F_3$. Its lattice dimensions are large, however, compared with those of $K_{0.50}Ni_{0.50}Cr_{0.50}F_3$ (Table I), and there are extra lines in its X-ray powder pattern. It is difficult to imagine that Na^+ ions could occupy anything but the tetrahedral sites, and as was the case for $K_{0.60}Ni_{0.60}V_{0.40}F_3$ described above, occupation of the tetrahedral sites increases the dimensions of the unit cell. The compounds $Na_{0.50}Ni_{0.50}Cr_{0.50}F_3$ and $Na_{0.50}Ni_{0.50}V_{0.50}F_3$ do not form the modified pyrochlore

structure, which probably means that at least some of the truncated tetrahedral sites are occupied by larger A^+ ions in order for the structure to form.

The modified pyrochlore and tetragonal tungsten bronze structures demonstrate how physical properties depend on structure. The most striking difference between the magnetic properties of the two structures (Table I) is the large negative Θ values of the modified pyrochlores as opposed to mostly small positive Θ values for the tetragonal bronze compounds. This difference is a consequence of the relative number of $M^{2+}-F^- - M^{2+}$, $M^{3+}-F^- - M^{3+}$, and $M^{2+}-F^- - M^{3+}$ near-neighbor interactions, which is 1:1:2 in the cubic, modified pyrochlore structure and 1:1:13 in the ordered, tetragonal bronze structure. It is because of the relatively large number of $M^{2+}-F^- - M^{3+}$ near-neighbor interactions (which are ferromagnetic) that the Θ values of the tetragonal bronze compounds are positive.

It is not surprising that long-range magnetic ordering was not observed in the modified pyrochlore phases since this structure gives rise to so many magnetic constraints (frustrations). Differences in the magnetic properties of $K_{0.50}Ni_{0.50}Cr_{0.50}F_3$ and $K_{0.50}Ni_{0.50}V_{0.50}F_3$, however, are surprising. From Figure 6, it appears that a considerable amount of magnetic coupling occurs in (Ni,V) near 100 K. We assume this is antiferromagnetic coupling between neighboring Ni^{2+} ions. What is strange is that no such effect is seen in (Ni,Cr). One possible explanation is that

(Ni,V) goes through some crystallographic phase change between 100 and 300 K.

Conclusions

The most important conclusion of this work is that $M^{2+}-M^{3+}$ ionic ordering is common in first-row transition metal fluorides having the tetragonal tungsten bronze structure. In $K_xMn_xCr_{1-x}F_3$, $K_xMn_xV_{1-x}F_3$, $K_{0.60}Ni_{0.60}Cr_{0.40}F_3$, and $Na_{0.25}K_{0.25}Mn_{0.50}Cr_{0.50}F_3$ $|J_{2+,2+}| \approx |J_{3+,3+}| \gg |J_{2+,3+}|$. This difference in magnitude of magnetic coupling energies causes magnetic ordering to occur in steps. Although neutron diffraction studies are necessary to unambiguously confirm the magnetic structures, it appears that linear trimers form first, giving rise to a quasi-paramagnetic region, followed by long-range magnetic ordering at a lower temperature. The 180° $M^{2+}-F^- - M^{3+}$ interactions ($M^{2+} = Mn, Ni; M^{3+} = V, Cr$) are ferromagnetic. The modified pyrochlore structure sometimes forms with smaller alkali metal ions like K^+ and Na^+ . At some compositions, these compounds form ordered structures of lower symmetry, although they remain cubic.

Acknowledgment. We gratefully acknowledge the National Science Foundation (Grants DMR 79-00313, DMR 76-83360, and DMR 77-11970) for financial support, including the purchase of major equipment, and The University of Mississippi for cost sharing. Appreciation is expressed to The University of Mississippi Computer Center for providing data reduction time.

Contribution from the Departamento de Química Inorgánica, Facultad de Ciencias, Universidad de Málaga, 29071 Málaga, Spain, and Department of Chemistry, University of Cambridge, Lensfield Road, Cambridge CB2 1EW, U.K.

Order and Disorder of Vanadyl Chains: Crystal Structures of Vanadyl Dihydrogen Arsenate $(VO(H_2AsO_4)_2)_2$ and the Lithium Derivative $Li_4VO(AsO_4)_2$

Miguel A. G. Aranda,[†] J. Paul Attfield,[‡] Sebastian Bruque,^{*,†} and Maria Martinez-Lara[†]

Received July 10, 1991

The crystal structure of layered, tetragonal $VO(H_2AsO_4)_2$ ($a = 9.1305$ (1) Å, $c = 8.1318$ (2) Å) has been refined in space group $I4/mcm$ from laboratory X-ray powder diffraction data by the Rietveld method, giving $R_{wp} = 10.1\%$ and $R_F = 5.5\%$. Disorder of the vanadium atoms over two sites results from infinite $\cdot V=O \cdots V=O \cdot$ chains orienting in the $\pm c$ -directions at random, due to the flexibility of the arsenate groups that link neighboring chains. The two modes of ordering the vanadyl chains to give structures with $P4/ncc$ and $I4cm$ symmetry, both of which have been reported, are also discussed. The structure of the lithium derivative $Li_4VO(AsO_4)_2$ ($a = 9.0293$ (2) Å, $c = 9.0053$ (4) Å), obtained by ion exchange, has $P4/ncc$ symmetry due to partial ordering between vanadyl chains and has been refined to $R_{wp} = 13.8\%$ and $R_F = 9.3\%$. The lithium ions occupy irregular five-coordinate sites between vanadyl arsenate layers. The different behavior of the $VO(H_2XO_4)_2$ compounds ($X = P, As$) toward ionic exchange reactions is discussed in the light of these results.

Introduction

Vanadium phosphorus oxides have a rich and complex structural chemistry owing to the variable oxidation state of vanadium and the variety of observable phosphorus to vanadium ratios. These compounds have been extensively studied due to their interesting catalytic properties¹⁻³ and their ability to act as host materials for ion exchange and intercalation reactions.^{4,5} Butane and butene can be oxidized to maleic anhydride with air over vanadium phosphate catalysts.^{6,7} The consensus of the studies is that the best catalysts have vanadium in the +4 oxidation state and a P/V ratio of approximately 1 and $(VO)_2P_2O_7$, which exhibits these values, has been detected in active catalysts with high selectivities.

Although vanadium phosphates have been widely studied,⁸ possible arsenic analogues have received less attention. We have recently reported the synthesis and characterization of vanadyl dihydrogen arsenate $VO(H_2AsO_4)_2$ and the lithium derivative $Li_4VO(AsO_4)_2$ obtained by a "chimie douce" reaction.⁹ The crystal structure of the apparently isostructural vanadyl dihydrogen phosphate, $VO(H_2PO_4)_2$, has been reported,¹⁰ but according to

the literature this compound does not exchange H^+ with Li^+ or other cations.¹¹ We have therefore investigated the structures of $VO(H_2AsO_4)_2$ and $Li_4VO(AsO_4)_2$ to clarify the differences between the crystal chemistries and ion-exchange reactions of the arsenate and phosphate compounds.

Experimental Section

The synthesis and chemical analysis of $VO(H_2AsO_4)_2$ and $Li_4VO(AsO_4)_2$ were carried out as described elsewhere.⁹ Both preparations

- (1) Bordes, E.; Courtine, P. *J. Catal.* **1979**, *57*, 236.
- (2) Hodnett, B. K.; Delmon, B. *Appl. Catal.* **1983**, *6*, 245.
- (3) Poli, G.; Resta, I.; Ruggeri, O.; Trifiro, F. *Appl. Catal.* **1981**, *1*, 375.
- (4) Martinez-Lara, M.; Jimenez-Lopez, A.; Moreno-Real, L.; Bruque, S.; Casal, B.; Ruiz-Hitzky, E. *Mater. Res. Bull.* **1988**, *20*, 549.
- (5) Ladwig, G. Z. *Anorg. Allg. Chem.* **1965**, *338*, 266.
- (6) Hodnett, B. K.; Permann, P.; Delmon, B. *Appl. Catal.* **1983**, *6*, 231.
- (7) Vartuli, J. C.; Zener, J. R.; U.S. Patent 4247 419, 1981.
- (8) Beltran-Porter, D.; Beltran-Porter, A.; Amoros, P.; Ibanez, R.; Martinez, E.; Le Bail, A.; Ferey, C.; Villeneuve, G. *Eur. J. Solid State Inorg. Chem.* **1991**, *28*, 131.
- (9) Martinez-Lara, M.; Bruque, S.; Moreno, L.; Aranda, M. A. G. *J. Solid State Chem.* **1991**, *91*, 25.
- (10) Linde, S. A.; Gorbunova, Y. E.; Lavrov, A. V.; Kuznetsov, V. G. *Dokl. Akad. Nauk SSSR* **1979**, *244*, 1411.
- (11) Ladwig, G. Z. *Chem.* **1968**, *8*, 307.

[†] Universidad de Málaga.

[‡] University of Cambridge.